I&EC research
Industrial & Engineering Chemistry Research

Article

pubs.acs.org/IECR

Incorporating Fouling Modeling into Shell-and-Tube Heat Exchanger Design

Andressa Nakao,[†] Andrea Valdman,[†] André L. H. Costa,[‡] Miguel J. Bagajewicz,[§] and Eduardo M. Queiroz*,[†]

[†]Escola de Química CT, Federal University of Rio de Janeiro (UFRJ), Bloco E, Ilha do Fundão, Rio de Janeiro, Rio de Janeiro CEP 21949-900, Brazil

[‡]Institute of Chemistry, Rio de Janeiro State University (UERJ), Rua São Francisco Xavier, 524, Maracanã, Rio de Janeiro, Rio de Janeiro CEP 20550-900, Brazil

[§]School of Chemical, Biological and Materials Engineering, University of Oklahoma, Norman, Oklahoma 73019, United States

ABSTRACT: Fouling is a major problem in the operation of heat exchangers, resulting in increased capital, operational, and maintenance costs. Shell-and-tube heat exchangers are traditionally designed using fixed values of fouling resistances, ignoring that fouling rates depend on the exchanger geometry, rendering different fouling resistances for the same thermal service. This article discusses the use of fouling rate models in the design of shell-and-tube heat exchangers. We link a heat exchanger design algorithm to a dynamic simulation of the fouling rate. The proposed procedure is explored for the design of heat exchangers where fouling occurs in the tube side due to crude oil flow. Four examples illustrate how the utilization of the fouling rate model alters the solution of the design problem, including aspects related to a "no fouling" condition in the design, the impact of the duration of the operational campaign in the results, and how the uncertainty in the fouling prediction can be handled.

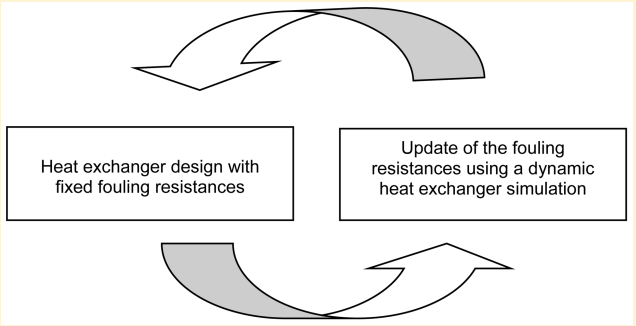

1. INTRODUCTION

Due to the structural simplicity, flexibility, and robustness, shell-and-tube heat exchangers are the most common heat transfer alternative used in power plants, oil refineries, and chemical plants.

The shell-and-tube heat exchanger design problem includes several interdependent qualitative and quantitative elements. Traditionally, it is a procedure strongly based on the designer experience. Nowadays, there are several commercial software programs available to assist heat exchanger designers, such as HTRI, and Aspen Shell and Tube Exchanger. These tools contain algorithmic routines that may provide automatic solutions for the heat exchanger design problem.[1] Additionally, the literature contains a considerable number of papers that employs optimization tools for the solution of the design problem. These procedures involve a diversity of approaches, encompassing a variety of objective functions, design variables, and optimization methods. The solution techniques investigated include mathematical programming,[2−4] stochastic methods,[5,6] and heuristic methods.[7]

However, independently of the approach, the fouling problem is usually considered in the design using fixed fouling factors, which estimate the impact of the deposits in the heat exchanger performance. Despite the development of fouling rate models, the utilization of model predictions in the design is relatively scarce in the literature. Butterworth[8] explored the utilization of the fouling rate in the heat exchanger design through three approaches: (a) searching for the design associated with "no fouling" conditions; (b) design of the heat exchanger using an asymptotic value of the fouling resistance based on a rate model; and (c) exploring the fouling rate in the design according to an assumed operational history. The design analysis is conducted based on a graphical representation of the feasible solutions in relation to the number and length of the tubes. The same graph was also employed by Polley et al.[9] to analyze how different alternatives of shell and tube heat exchangers are affected by fouling in the design. Nesta and Bennet[10] presented guidelines to be employed in the design of a heat exchanger to suppress fouling. Finally, Caputo et al.[11] presented a heat exchanger design method, where the exchanger optimization is made with maintenance considerations. In their approach, the authors include the cleaning schedule cost in the final cost and define a maximum allowable fouling resistance during the operating time. An empirical fouling model, dependent on the flow velocity, is employed for estimating the fouling resistance values during the period between cleaning shutdowns.

Received: September 14, 2016
Revised: March 16, 2017
Accepted: March 22, 2017
Published: March 22, 2017

DOI: 10.1021/acs.iecr.6b03564
Ind. Eng. Chem. Res. 2017, 56, 4377−4385

Aiming at contributing to this effort of inserting the fouling phenomenon in the design beyond the conventional fixed fouling resistances, this paper presents a design procedure where the fouling resistance is calculated based on the thermofluidynamic conditions of the design itself. This interrelation is provided by coupling the design algorithm to a dynamic simulation (pseudostationary) of the heat exchanger subjected to fouling. The convergence between the fouling resistance used in the design and the final fouling resistance in the simulation is promoted by an external loop. Among the different fouling problems, this paper presents the proposed procedure applied to chemical reaction fouling in crude oil streams.

The article is organized as follows. Section 2 describes the fouling modeling associated with the design, Section 3 presents the heat exchanger simulation using the fouling rate model, Section 4 presents the proposed procedure of interconnection between the design algorithm and the fouling rate model, Section 5 explores the proposed procedure through four examples, and Section 6 presents the conclusions.

2. FOULING MODELING

In heat transfer technology, fouling is the undesired accumulation of deposits over the thermal surface of heat exchanger equipment. It causes an increase of capital, operating, and maintenance costs. Its usage in heat exchanger design is based on the insertion of additional resistances in the thermal circuit between the hot and the cold streams. The overall heat transfer coefficient in the design considering the presence of fouling (U_{dirty}) encompasses the convective heat transfer resistances, the wall conductive resistance, and the resistances associated with fouling and is given by

$$U_{dirty} = \frac{1}{\frac{1}{h_t}\left(\frac{dte}{dti}\right) + Rf_t\left(\frac{dte}{dti}\right) + \frac{dte\ \ln(dte/dti)}{2ktube} + Rf_s + \frac{1}{h_s}} \quad (1)$$

where h_t and h_s are the convective heat transfer coefficients in the tube side and shell side, dte and dti are the outer and inner tube diameters, ktube is the thermal conductivity of the tube wall, and Rf_t and Rf_s are the fouling resistances associated with the tube-side and shell-side streams.

This expression can be related to the overall heat transfer condition in the clean condition (U_{clean}):

$$U_{dirty} = \frac{1}{\frac{1}{U_{clean}} + Rf} \quad (2)$$

where Rf encompasses the fouling resistances of both streams.

Fouling resistances imply a higher heat transfer area needed in the design to guarantee that the heat exchanger will attain the needed heat load according to the process specifications during the entire period between cleaning shutdowns. If the fouling resistance presents an asymptotic behavior, the adequate insertion of the fouling resistance would allow the continuous operation of the heat exchanger without cleaning. Typical values of fouling resistances can be found in tables available in the literature. Usually, in these tables, the values of the fouling resistance are only associated with the nature of the stream for the majority of the fluids. In more specific tables (e.g., TEMA), for some specific fluids (e.g., water and crude oil), the fouling resistance values are associated with ranges of flow velocity and fluid temperature.

The central idea of the current paper is to employ fouling rate models to determine the fouling resistance to be used in the design. The fouling rate model employed must be able to describe the impact of the thermofluidynamic conditions on fouling for each design alternative (e.g., two design solutions associated with distinct values of flow velocities must present different values of fouling resistances for the same service).

The first rate model describing fouling behavior was developed by Kern and Seaton in 1959.[12] The model considers fouling as a result of two simultaneous processes, a deposition process and a removal process:

$$\frac{dRf}{dt} = \varphi_D - \varphi_R \quad (3)$$

where φ_D and φ_R are the deposition and removal rates, respectively.

Because of fouling may be associated with different causes (sedimentation, precipitation, chemical reaction, biological growth, corrosion, and freezing), the phenomenological determination of the deposition and removal rates depends on the specific nature of the streams flowing in the heat exchanger. In this context, the present design procedure can be employed using any fouling rate model dependent on the thermofluidynamic conditions. Particularly, the analysis presented here is focused on crude oil fouling associated with the presence of asphaltenes (chemical reaction fouling).

There are three approaches for fouling rate models in crude oil streams: (i) deterministic; (ii) semiempirical; and (iii) artificial neural network.[13] In the deterministic approach, some researchers have presented fouling rate models based on physical analysis, similar to particulate and crystallization fouling studies, but due to the complexity of the crude oil nature, these models lost importance. The semiempirical approach includes the effects of the operational variables (e.g., flow velocity and film/wall temperature) for the fouling rate description, where the model parameters must be determined through parameter estimation procedures using experimental or plant data. The last approach incorporates statistical learning algorithms creating relationships between different variables related to fouling phenomenon.

Among the existent alternatives, semiempirical models using the threshold fouling concept of Ebert and Panchal assume a central role in the literature.[14] The Ebert and Panchal model describes fouling as a phenomenon controlled by two mechanisms that compete between themselves, deposition and suppression, indicating the possibility of a "no fouling condition" where these two mechanisms cancel each other out.[15] This concept is the base of several later similar models.[16−18]

Among the different alternatives, the Ebert−Panchal modified fouling rate model is used in this paper,[16] with the suggestion of Lestina and Zettler[19] to employ the surface temperature instead of the film temperature:

$$\frac{dRf}{dt} = \alpha Re^{-0.66} Pr^{-0.33} \exp\left(-\frac{E_a}{RT_{surf}}\right) - \gamma\tau_w \quad (4)$$

where Re and Pr represent the Reynolds and the Prandtl numbers, R is the universal gas constant, T_{surf} is the fouling surface absolute temperature, τ_w is the shear stress, and α and γ are empirical model parameters which, together with the fouling activation energy (E_a), must be estimated based on

DOI: 10.1021/acs.iecr.6b03564
Ind. Eng. Chem. Res. 2017, 56, 4377−4385

experimental or plant data. The shear stress can be calculated by

$$\tau_w = f\rho\frac{v^2}{2} \tag{5}$$

where f is the Fanning friction factor, ρ is the density, and v is the mean flow velocity. The friction factor expression can be given by[20]

$$f = 0.0035 + \frac{0.264}{Re^{0.42}} \tag{6}$$

The first term in the RHS of eq 4 corresponds to the deposition, and the second term represents suppression. The interpretation of the negative term as a suppression effect instead of the traditional Kern and Seaton's removal is still the object of discussion in the literature. The suppression effect is associated with the deposition inhibition due to fluidynamic effects or diffusion of the foulant to the bulk. The removal effect corresponds to the erosion or tear of the deposit caused by the shear stress.[21]

Using the fouling rate equation, the threshold concept can be graphically described by a fouling envelope, as it is illustrated in Figure 1. This envelope allows the observation of fouling and no fouling regions.

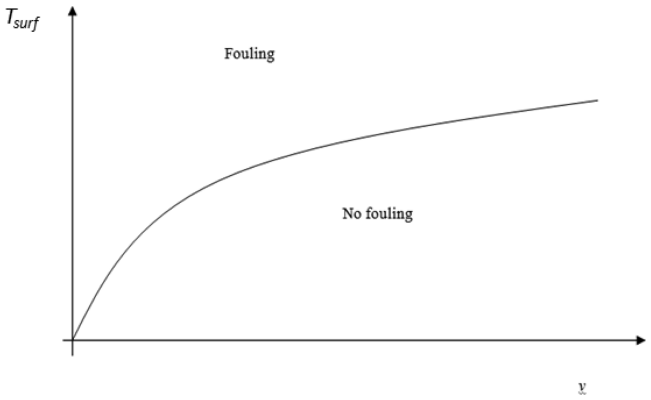

Figure 1. Representation of the threshold concept in relation to the surface temperature (T_{surf}) and the flow velocity (v).

3. HEAT EXCHANGER SIMULATION

The analysis of the heat exchanger behavior affected by fouling associated with the design algorithm involves its simulation during the period between cleaning shutdowns. Since fouling is a slow process, the dynamic simulation of the heat exchanger can be done using a pseudostationary model. The resultant mathematical model is composed of the fouling rate differential equation together with algebraic equations of the steady-state model using the ε-NTU method and an equation for evaluation of the fouling surface temperature. The reduction of the inner diameter due to the fouling thickness growth is not considered in the model.

3.1. Fouling Rate. According to the previous section, the fouling rate model employed is the modified Ebert−Panchal model, with fouling only occurring in the tube side of crude oil heating (this hypothesis is usually adopted in the analysis of fouling in crude preheat trains[22]). Along the heat exchanger area, the stream temperature profiles imply that each point of the heat exchanger presents a different fouling rate. Aiming to avoid a more complex model (which would involve additional differential equations), the spatial variation of the fouling rate is substituted by an average value calculated using the fouling rates at the heat exchanger ends in an equivalent countercurrent configuration:

$$\left(\frac{dRf}{dt}\right)_{avg} = \frac{1}{2}\left[\left(\frac{dRf}{dt}\right)_1 + \left(\frac{dRf}{dt}\right)_2\right] \tag{7}$$

where the subscripts 1 and 2 indicate the heat exchanger ends. A more accurate alternative that could be also employed for the determination of the average fouling rate is described in Ishiyama et al.[23]

Adopting the suppression hypothesis,[13,15] the fouling rate will never assume negative values; i.e., it is considered that the shear stress would not be able to remove any existent deposits. Therefore, the final form of the fouling rate model becomes

$$\frac{dRf}{dt} = \max\left(0, \left(\frac{dRf}{dt}\right)_{avg}\right) \tag{8}$$

Despite the fact that the model described involves only tube-side fouling, the proposed procedure could accommodate fouling in the tube side and shell side simultaneously. In this case, instead of a single differential equation, there would be a system with two differential equations to solve.

3.2. Steady-State Heat Exchanger Equations. The heat exchanger model employs the ε-NTU method.[24] This method contains three dimensionless variables: the effectiveness (ε), the number of transfer units (NTU), and the ratio between heat capacity flow rates (C_R):

$$\varepsilon = \frac{Q}{Q_{max}} \tag{9}$$

$$\mathrm{NTU} = \frac{U_{foul}A}{C_{min}} \tag{10}$$

$$C_R = \frac{C_{min}}{C_{max}} \tag{11}$$

where Q is the heat load, Q_{max} is the maximum heat load thermodynamically possible, U_{foul} is the fouled overall heat transfer coefficient at a given moment, A is the heat transfer area, and C_{min} and C_{max} are the heat capacity flow rates (mCp) of the minimum and maximum fluids (respectively, the streams with the higher and lower heat capacity flow rates). The fouled overall heat transfer coefficient is calculated using the value of the fouling resistance at the respective instant of the integration path.

The thermodynamic limit of the heat load is given by

$$Q_{max} = C_{min}(T_{h,i} - T_{c,i}) \tag{12}$$

where $T_{h,i}$ and $T_{c,i}$ are the inlet temperatures of the hot and cold streams, respectively.

Using energy balances and the heat transfer rate equation, it is possible to establish a relationship among these three variables:

$$\varepsilon = \varepsilon(\mathrm{NTU}, C_R) \tag{13}$$

The ε-NTU relations are available for each specific heat exchanger configuration. For example, the ε-NTU relation for a heat exchanger with a countercurrent configuration is

DOI: 10.1021/acs.iecr.6b03564
Ind. Eng. Chem. Res. 2017, 56, 4377−4385

$$\varepsilon = \frac{1 - \exp[-\mathrm{NTU}(1 - C_R)]}{1 - C_R \exp[-\mathrm{NUT}(1 - C_R)]} \quad (14)$$

The outlet temperatures of the heat exchanger can be evaluated from the effectiveness. If the hot stream is the minimum fluid (i.e., the stream with the smaller heat capacity flow rate), as usually occurs in crude preheat trains, the corresponding equations for the evaluation of the outlet temperatures are

$$T_{h,o} = T_{h,i} - \frac{\varepsilon Q_{max}}{C_{min}} \quad (15)$$

$$T_{c,o} = T_{c,i} + \frac{\varepsilon Q_{max}}{C_{max}} \quad (16)$$

Equivalent equations can be deducted when the cold stream is the minimum fluid.

3.3. Surface Temperature Equation. The temperature of the surface in contact with the cold stream can be calculated through the thermal circuit between hot and cold streams:

$$\frac{T_h - T_{surf}}{\frac{1}{h_s \mathrm{dte}} + \frac{\ln(\mathrm{dte}/\mathrm{dti})}{2\mathrm{ktube}} + \frac{Rf}{\mathrm{dti}}} = \frac{T_{surf} - T_c}{\frac{1}{h_t \mathrm{dti}}} \quad (17)$$

4. EXCHANGER DESIGN AND FOULING RATE MODELING

The proposed procedure is composed of two main steps: the design algorithm and the heat exchanger simulation. This analysis can employ any heat exchanger design algorithm available, where it is illustrated here the utilization of the design option of the HTRI software.

First, the HTRI design tool is used to obtain a shell-and-tube heat exchanger design candidate for the required service based on an estimated fouling resistance (e.g., TEMA value). To run this step, a set of parameters must be defined by the engineer: fluid allocation (tube or shell), materials (shell, tube, etc.), shell and head types, baffle type and cut, tube pitch ratio, tube layout pattern, outer tube diameter, and tube wall thickness. The searched parameters by the software in the design are inner shell diameter, total number of tubes, number of tube passes, tube length, and baffle spacing.

After the design made by HTRI, the corresponding heat exchanger is simulated for the planned operational run between cleaning shutdowns. The convective heat transfer coefficients employed in the simulation are extracted from the HTRI run; therefore, despite the utilization of analytical solutions based on the ε-NTU method, it is possible to assume the accuracy of the results.

The final value of the fouling resistance is then compared with the initial estimate (see Figure 2). If the values are similar, according to a certain tolerance, the procedure is finished; otherwise, the HTRI is executed again with the new value of the fouling resistance. The steps are repeated until convergence is achieved.

Computational tests have indicated that sometimes convergence is not reached; therefore, another stopping criterion is included in the algorithm based on the maximum number of iterations. The analysis of the results of the search in the nonconverged cases indicates a cyclic repetition of a sequence of fouling resistances. In these cases, the design solution corresponds to the alternative associated with the smallest value

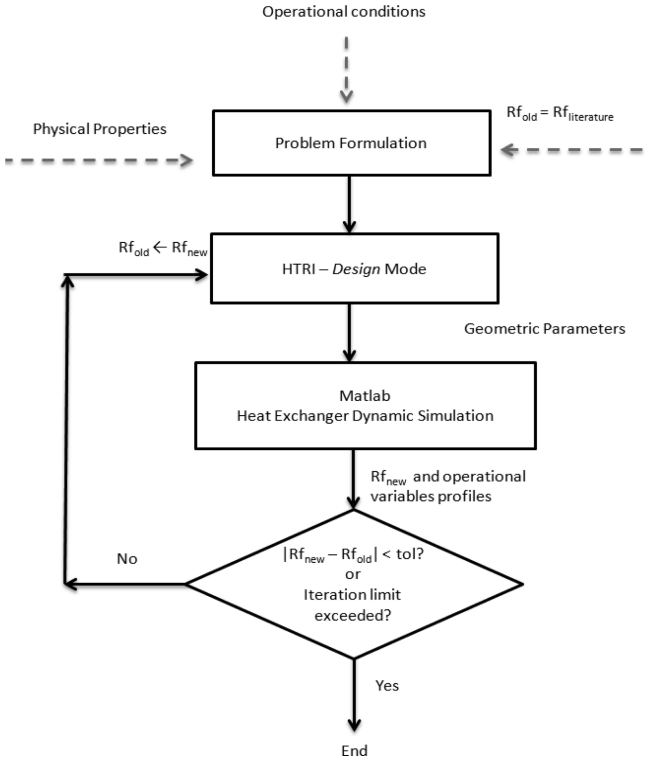

Figure 2. Design procedure using fouling rate modeling.

of input fouling resistance, which yields in the dynamic simulation a lower final fouling resistance; i.e., the solution presents a design fouling resistance higher than the maximum value reached during the simulation, thus guaranteeing a feasible design according to the fouling rate model.

The convergence scheme runs automatically in the Matlab software (version R2009b). The code includes subroutines for the communication between Matlab and HTRI and subroutines to solve the differential-algebraic system of equations, using the DASSL solver.

5. EXAMPLES

In order to show the performance of the proposed procedure, three examples are investigated, representing crude preheat train exchangers without phase change. These examples represent the same design task but involving different sets of fouling rate parameters. These values are shown in Table 1, coherent with the range displayed in Wilson et al.[13]

Table 1. Fouling Rate Model Parameters (Equation 4)

	Example 1	Example 2	Example 3
α (m^2·K/J)	1.078	13.97	7.360
E_a (kJ/mol)	50.0	48.0	65.5
γ (m^2·K/(J·Pa))	4.03×10^{-11}	3.44×10^{-8}	4.17×10^{-12}

The set of examples presents different aspects of the solutions that the design procedure can reach. Example 1 explores a design solution where the proposed algorithm converges for a given value of fouling resistance predicted by the fouling rate model, Example 2 presents a problem with a "no fouling" solution, Example 3 explores the impact in the design of different operational periods between cleaning

DOI: 10.1021/acs.iecr.6b03564
Ind. Eng. Chem. Res. 2017, 56, 4377−4385

shutdowns, and Example 4 is employed to discuss the uncertainty associated with the fouling model.

The basic specifications of the heat exchanger design are depicted in Table 2, the search space is described in Table 3,

Table 2. Basic Specifications of the Heat Exchangers

	specification
TEMA type	AES
baffle type	single segmental
baffle cut (%)	25.0
tube pitch ratio	1.25
tube layout	triangular
outer tube diameter (mm)	19.0
tube thickness (mm)	2.1

Table 3. Input Specifications in the HTRI Design Mode

	specification
number of tube passes	1, 2, 4, 6, ...
tube length (m)	4.00, 4.50, 5.00, 5.50, 6.00
overdesign (%)	0.00 to 10.0
tube side velocity bounds (m/s)	1.00 to 3.00
shell side velocity bounds (m/s)	0.50 to 2.00

Table 4. Specifications of the Streams

	hot stream	cold stream
mass flow rate (kg/s)	45.0	95.0
inlet temperature (°C)	255	165
outlet temperature (°C)	229	180
density (kg/m^3)	852	819
heat capacity (kJ/(kg·K))	2.90	2.40
viscosity (Pa·s)	1.70×10^{-3}	1.30×10^{-3}
thermal conductivity (W/(m·K))	0.11	0.10
allowable pressure drop (kPa)	70	70

and the data of the streams are shown in Table 4. The dynamic simulations are conducted considering a two year period between cleanings for Examples 1 and 2. Examples 3 and 4 involve operation campaigns with different durations. The tolerance adopted in the convergence is 10^{-5} m^2·K/W. The initial value of the fouling resistance adopted in the search is based on the TEMA value, consistent with the crude heating design task: dry crude, velocity higher than 1.2 m/s, and temperature range between 121 and 177 °C.[25]

5.1. Example 1. The application of the proposed procedure obtained a solution after four iterations. Table 5 presents the design solution found (Final design). This table also depicts the initial heat exchanger designed using the TEMA fouling factor (TEMA design). The design fouling resistance presented in Table 5 corresponds to the value employed in the HTRI input, and the simulated fouling resistance is the corresponding value at the end of the simulation. The thermofluidynamic data of the solutions are shown in Table 6.

Table 5. Example 1—Heat Exchanger Design Solutions

	TEMA design	final design
design fouling resistance (m^2·K/W)	0.00035	0.00007
simulated fouling resistance (m^2·K/W)	0.00113	0.00007
area (m^2)	76.8	62.7
total number of tubes	235	235
number of tube passes	1	1
shell diameter (m)	0.438	0.438
tube length (m)	5.50	4.50
baffle spacing (m)	0.394	0.370

Table 6. Example 1—Heat Exchanger Design Solutions: Thermofluidynamic Variables

	initial design	final design
overall heat transfer coefficient (W/(m^2·°C))	661	866
tube-side film coefficient (W/(m^2·°C))	2340	2359
shell-side film coefficient (W/(m^2·°C))	2119	2124
tube-side flow velocity (m/s)	2.86	2.86
shell-side flow velocity (m/s)	0.96	1.00
tube-side pressure drop (kPa)	43.9	37.5
shell-side pressure drop (kPa)	66.0	58.6

The comparison between both solutions indicates that the proposed procedure was able to modify the initial design according to the fouling rate model predictions. The equivalence of the design and simulated fouling resistances in the final design show the convergence of the algorithm, according to the tolerance selected.

Starting from the TEMA fouling resistance value, the algorithm identifies a heat exchanger with an area 18.3% smaller, based on the fouling rate model attached to the design algorithm.

Profiles of the simulation of the final design solution are presented in Figures 3, 4, and 5. These figures show a

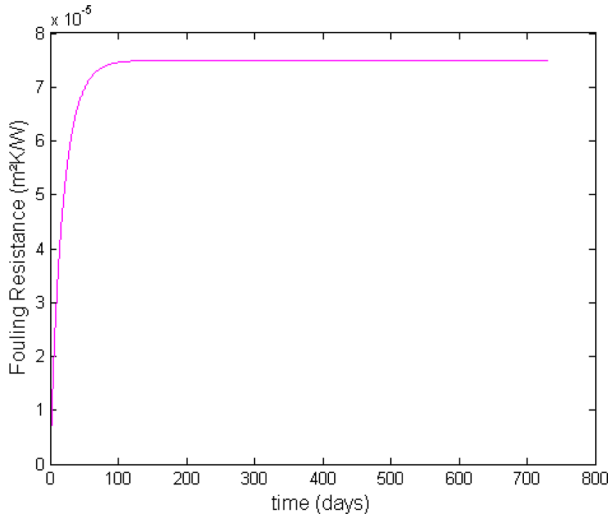

Figure 3. Fouling resistance profile of Example 1.

continuous increase of the fouling resistance, associated with the corresponding modification of the outlet temperatures, until an asymptotic value is virtually reached. This asymptotic pattern occurs because the deposit accumulation tends to decrease the surface temperature in contact with the crude oil; therefore, the deposition term in the Ebert–Panchal model decreases with time, becoming equal to the suppression term, which implies a null fouling rate.

It is important to observe that the values of the temperatures determine a heat load during the entire period higher than the service specification.

DOI: 10.1021/acs.iecr.6b03564
Ind. Eng. Chem. Res. 2017, 56, 4377–4385

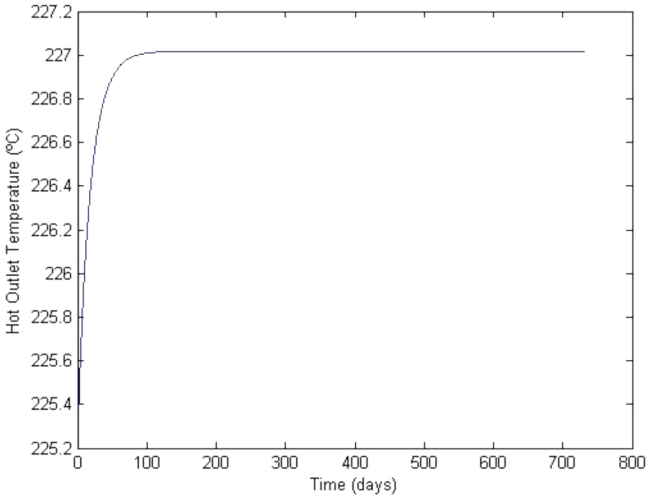

Figure 4. Outlet temperature of the hot stream in Example 1.

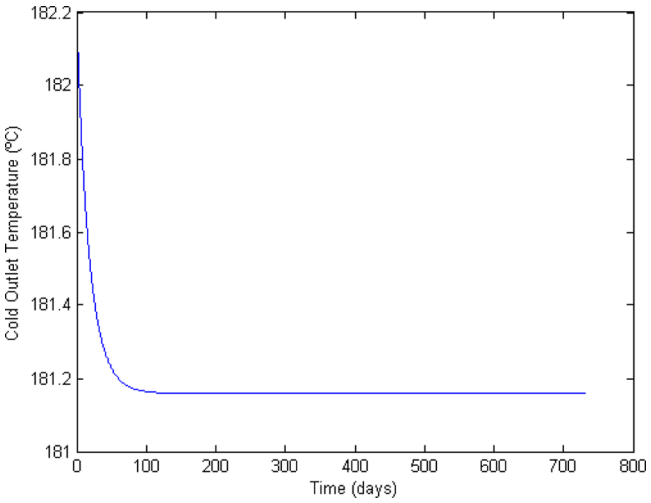

Figure 5. Outlet temperature of the cold stream in Example 1.

5.2. Example 2. The initial and final design solutions are presented in Table 7. The thermofluidynamic data of the solutions are shown in Table 8. The convergence is reached in two iterations. An interesting fact that can be observed here is the absence of fouling in the final design, i.e., the proposed procedure was able to identify a "no fouling" solution. Based on this fact, the HTRI software provided a heat exchanger with an area 27% smaller. Additionally, the no fouling behavior would allow the continuous operation of the heat exchanger without the need of cleaning actions.

Table 7. Example 2—Heat Exchanger Design Solutions

	TEMA design	final design
design fouling factor (m^2·K/W)	0.00035	0.00000
simulated fouling factor (m^2·K/W)	0.00000	0.00000
area (m^2)	76.8	55.7
total number of tubes	235	235
number of tube passes	1	1
shell diameter (m)	0.438	0.438
tube length (m)	5.50	4.00
baffle spacing (m)	0.394	0.315

Table 8. Example 2—Heat Exchanger Design Solutions: Thermofluidynamic Variables

	initial design	final design
overall heat transfer coefficient (W/(m^2·°C))	661	956
tube-side film coefficient (W/(m^2·°C))	2340	2367
shell-side film coefficient (W/(m^2·°C))	2119	2172
tube-side flow velocity (m/s)	2.86	2.86
shell-side flow velocity (m/s)	0.96	1.12
tube-side pressure drop (kPa)	43.9	34.3
shell-side pressure drop (kPa)	66.0	65.4

The fouling envelope related to the threshold concept is illustrated in Figure 6, where it is possible to observe that the final design solution is inside the no fouling region.

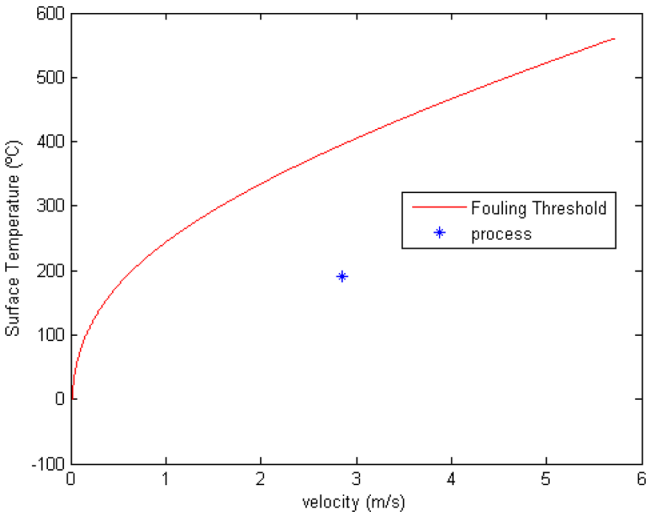

Figure 6. Fouling envelope of Example 2.

5.3. Example 3. The proposed design procedure was applied considering three different campaigns between cleanings: 6 months, 2 years, and 4 years. The corresponding solutions together with the initial heat exchanger designed using the TEMA fouling factor (TEMA design) are shown in Table 9. The thermofluidynamic data of the solutions are present in Table 10.

The comparison of the results shows that the increase of the campaign duration implies in an augmentation of the final fouling resistance in the solution. The design alternatives considering 2 years and 4 years of campaign present fouling resistances 62% and 75% higher than the 6 months design option, respectively. Consequently, the corresponding design solutions present overall heat transfer coefficients 12% and 15% lower. This reduction of the overall heat transfer coefficient determines an increase of the area with the duration of the campaign, where the proposed procedure identifies solutions with crescent tube lengths.

Figure 7 displays the temporal profiles of the fouling resistances according to each campaign. It can be observed that for the shorter campaigns, the fouling rate at the end of the period is not zero. Therefore, if the cleaning schedule is delayed in these cases, the heat exchanger would face higher fouling resistances than those established in the design. In practice, the problem is solved with more frequent cleaning and/or with additional fuel consumption in the fired heater at the end of the crude preheat train.

DOI: 10.1021/acs.iecr.6b03564
Ind. Eng. Chem. Res. 2017, 56, 4377−4385

Table 9. Example 3—Heat Exchanger Design Solutions: Design Variables

	TEMA design	6 month design	2 year design	4 year design
design fouling factor (m^2·K/W)	0.00035	0.00024	0.00039	0.00042
simulated fouling factor (m^2·K/W)	0.00042	0.00024	0.00039	0.00042
area (m^2)	76.8	69.7	76.8	83.8
total number of tubes	235	235	235	235
number of tube passes	1	1	1	1
shell diameter (m)	0.438	0.438	0.438	0.438
tube length (m)	5.50	5.00	5.50	6.00
baffle spacing (m)	0.393	0.426	0.393	0.440

Table 10. Example 3—Heat Exchanger Design Solutions: Thermofluidynamic Variables

	initial design	6 month design	2 year design	4 year design
overall heat transfer coefficient (W/(m^2·°C))	661	727	639	617
tube-side film coefficient (W/(m^2·°C))	2340	2347	2338	2336
shell-side film coefficient (W/(m^2·°C))	2119	2073	2118	2075
tube-side flow velocity (m/s)	2.86	2.86	2.86	2.86
shell-side flow velocity (m/s)	0.96	0.90	0.96	0.88
tube-side pressure drop (kPa)	43.9	40.7	43.9	47.1
shell-side pressure drop (kPa)	66.0	53.2	66.0	61.1

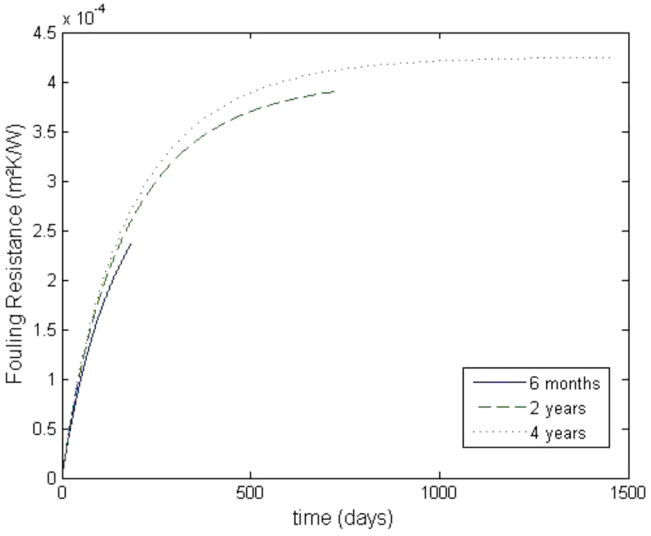

Figure 7. Fouling resistance profiles of Example 3.

This analysis indicates that the inclusion of the fouling rate model in the design procedure also allows the investigation of a trade-off involving capital costs and heat exchanger cleaning schedule. The increase of the time span between cleanings reduces costs associated with the maintenance activities and downtime but demands higher capital costs.[11]

5.4. Example 4. The fouling rate model parameters have some level of uncertainty. However, the literature does not provide a complete discussion about the uncertainty associated with fouling rate predictions. This example illustrates a case study with a simplified approach to handle this issue. Costa et al.[26] presented an investigation of the parameter estimation of semiempirical crude oil fouling rate models based on real data from a Brazilian refinery, where modified Ebert−Panchal model predictions implied in a mean absolute relative error (MAPE) of 7.1% between the model predictions and fouling resistance values obtained from plant data.[27] The analysis of the data sample employed indicates a standard deviation of the relative errors equivalent to 10%. Adopting this value to quantify the uncertainty associated with the fouling model predictions, we propose to conduct a sensitivity-based design procedure by multiplying the fouling values calculated by the heat exchanger simulation step by a factor equal to 1.2 (i.e., adding to the fouling resistance the double of the standard deviation calculated in Costa et al.[26]). Treatment of uncertainty more in depth requires the use of two-stage stochastic models that are outside the scope of this work and is part of future work.

This procedure was applied to the design problem associated with Example 1 and Example 3 with 2- and 4-year campaigns. The solution of the design problem of Example 1 was not modified, but Example 3, for both campaigns, resulted in larger heat exchangers (in order to avoid a two shell solution, the maximum allowable tube length was increased to 8 ft in the 4-year campaign case). Table 11 presents the solutions, and the corresponding thermofluidynamic data are present in Table 12.

Table 11. Example 4—Heat Exchanger Design Solutions

	2 year design	4 year design
design fouling resistance (m^2·K/W)	0.00049	0.00054
simulated fouling resistance (m^2·K/W)	0.00049	0.00054
area (m^2)	83.8	90.8
total number of tubes	235	235
number of tube passes	1	1
shell diameter (m)	0.438	0.438
tube length (m)	6.00	6.50
baffle spacing (m)	0.439	0.583

Table 12. Example 4—Heat Exchanger Design Solutions: Thermofluidynamic Variables

	2 year design	4 year design
overall heat transfer coefficient (W/(m^2·°C))	584	563
tube-side film coefficient (W/(m^2·°C))	2333	2331
shell-side film coefficient (W/(m^2·°C))	2074	2038
tube-side flow velocity (m/s)	2.86	2.86
shell-side flow velocity (m/s)	0.88	0.78
tube-side pressure drop (kPa)	47.1	50.3
shell-side pressure drop (kPa)	61.1	62.0

The design solution of the Example 1 problem was not modified because the original value of the fouling resistance is relatively low (even considering the increased fouling, the thermal resistance associated with fouling is only 10% of the total resistance in the thermal circuit). Therefore, the original design was also able to execute the service in the higher fouling resistance scenario. In the two cases explored in Example 3, the

DOI: 10.1021/acs.iecr.6b03564
Ind. Eng. Chem. Res. 2017, 56, 4377−4385

higher fouling resistances determined heat exchangers with areas 9% and 8% larger to fulfill the thermal task when the uncertainty treatment is applied.

6. CONCLUSIONS

Conventional heat exchanger design approaches involve the examination of different alternatives toward feasible and cheaper solutions. During the search, all the solution candidates present the same previously established fouling resistances, independently of the thermofluidynamic variables, especially flow velocity and surface temperature. However, this approach contains a considerable level of inaccuracy, because different heat exchangers proposed for the same service will present different levels of fouling.

The availability of fouling rate models that can predict the impact of the thermofluidynamic conditions on fouling offers the opportunity, explored in the current paper, to propose more effective design schemes for handling this problem. In this context, this paper presents a proposal of interconnection between conventional design algorithms and fouling rate models. Therefore, it is possible to insert the behavior of the fouling phenomenon during the design phase of the heat exchanger, aiming at its mitigation.

The resultant design scheme is explored using a commercial software for generating the design and a computational routine for determination of the fouling resistance through the heat exchanger dynamic simulation. The entire procedure is executed automatically. The structure of the proposed procedure is flexible, and the commercial design software employed could be substituted by any of the available optimization algorithms based on fixed fouling resistances available in the literature.[2−7]

Computational tests using the modified Ebert−Panchal model indicated that the proposal is able to modify the design, exploring the predictions of the fouling rate. Considering the relevant economic losses associated with fouling, the procedure may be a promising contribution for handling this problem at design level. Further research may be devoted to include the design generation and the fouling evaluation in a single optimization problem.

AUTHOR INFORMATION

Corresponding Author

*(E.M.Q.) E-mail: mach@eq.ufrj.br.

ORCID

Miguel J. Bagajewicz: 0000-0003-2195-0833

Eduardo M. Queiroz: 0000-0002-9424-5900

Notes

The authors declare no competing financial interest.

ACKNOWLEDGMENTS

We would like to thank Professor André Luis Alberton by the discussions about the fouling rate model uncertainty.

NOMENCLATURE

A = area (m^2)
C_p = heat capacity (J/(kg·K))
C_{max} = heat capacity flow rate of the maximum fluid
C_{min} = heat capacity flow rate of the minimum fluid
C_R = ratio between heat capacity flow rates
dte = outer tube diameter (m)
dti = inner tube diameter (m)
E_a = activation energy (kJ/mol)
f = Fanning friction factor
h = convective heat transfer coefficient (W/(m^2·K))
L = tube length (m)
ktube = thermal conductivity of the tube wall (W/(m·K))
NTU = number of transfer units
Nu = Nusselt number
Pr = Prandtl number
Q = heat duty (W)
Q_{max} = maximum heat duty thermodynamically possible (W)
R = universal gas constant (J/(mol·K))
Rf = fouling factor (m^2·K/W)
Re = Reynolds number
t = time (s)
T = temperature (°C)
U = overall heat transfer coefficient (W/(m^2·K))
v = flow velocity (m/s)

Greek letters

α = Ebert and Panchal parameter (m^2·K/J)
ε = effectiveness
γ = Ebert and Panchal parameter (m^2·K/(J·Pa))
μ = dynamic viscosity (Pa·s)
ρ = density (kg/m^3)
τ_w = wall shear stress (Pa)

Subscripts

avg = average
c = cold stream
clean = no fouled
dirty = design dirty condition
foul = fouled
h = hot stream
i = inlet
o = outlet
s = shell
t = tube

REFERENCES

(1) Bell, K. J. Logic of the design process. In *Heat Exchanger Design Handbook*; Hewitt, G. F., Ed.; Begell House: 2008.

(2) Mizutani, F. T.; Pessoa, F. L. P.; Queiroz, E. M.; Hauan, S.; Grossmann, I. E. Mathematical Programming Model for Heat-Exchanger Network Synthesis Including Detailed Heat Exchanger Designs. 1, Shell-and-Tube Heat Exchanger Design. *Ind. Eng. Chem. Res.* **2003**, *42*, 4009−4018.

(3) Ravagnani, M. A. S. S.; Caballero, J. A. A MINLP model for the rigorous design of shell and tube heat exchangers using the Tema standards. *Chem. Eng. Res. Des.* **2007**, *85*, 1423−1435.

(4) Gonçalves, C. O.; Costa, A. L. H.; Bagajewicz, M. J. *AIChE J.* **2016**, DOI: 10.1002/aic.15556.

(5) Ponce-Ortega, J. M.; Serna-Gonzáles, M.; Jiménes-Gutiérrez, A. Use of genetic algorithms for optimal design of shell-and-tube heat exchangers. *Appl. Therm. Eng.* **2009**, *29*, 203−209.

(6) Sadeghzadeh, H.; Ehyaei, M. A.; Rosen, M. A. Techno-economic optimization of a shell and tube heat exchanger by genetic and particle swarm algorithms. *Energy Convers. Manage.* **2015**, *93*, 84−91.

(7) Costa, A. L. H.; Queiroz, E. M. Design optimization of shell-and-tube heat exchangers. *Appl. Therm. Eng.* **2008**, *28*, 1798−1805.

(8) Butterworth, D. Design of shell-and tube heat exchangers when the fouling depends on local temperature and velocity. *Appl. Therm. Eng.* **2002**, *22*, 789−801.

(9) Polley, G. T.; Wilson, D. I.; Yeap, B. L.; Pugh, S. J. Use of crude oil fouling threshold data in heat exchanger design. *Appl. Therm. Eng.* **2002**, *22*, 763−776.

(10) Nesta, J.; Bennet, C. A. Reduce fouling in shell-and-tube heat exchangers. *Hydrocarbon Process.* **2004**, *83*, 77−82.

DOI: 10.1021/acs.iecr.6b03564
Ind. Eng. Chem. Res. 2017, 56, 4377−4385

(11) Caputo, A. C.; Pelagagge, P. M.; Salini, P. Joint economic optimization of heat exchanger design and maintenance policy. *Appl. Therm. Eng.* **2011**, *31*, 1381−1392.
(12) Müller-Steinhagen, H. Heat Transfer Fouling: 50 Years After the Kern and Seaton Model. *Heat Transfer Eng.* **2011**, *32*, 1−13.
(13) Wilson, D. I.; Ishiyama, E. M.; Polley, G. T. Twenty years of Ebert and Panchal - What next? Presented at *Heat Exchanger Fouling and Cleaning Conference*, Dublin, Ireland, 2015.
(14) Ebert, W.; Panchal, C. B. Analysis of Exxon crude oil slip stream coking data. Presented at *Fouling Mitigation of Industrial Heat-Exchange Equipment*, San Luis Obispo, CA, U.S.A., 1995.
(15) Wilson, D. I.; Polley, G. T.; Pugh, S. J. Ten years of Ebert, Panchal and the "threshold fouling" concept. Presented at *Heat Exchanger Fouling and Cleaning Conference*, Kloster Irsee, Germany, 2005.
(16) Panchal, C. B.; Kuru, W. C.; Liao, C. F.; Ebert, W. A.; Palen, J. W. Threshold conditions of crude oil fouling. *Understanding Heat Exchanger Fouling and Mitigation*; Begell House: 1999.
(17) Polley, G. T.; Wilson, D. I.; Yeap, B. L.; Pugh, S. J. Evaluation of laboratory crude oil threshold fouling data for application to refinery pre-heat trains. *Appl. Therm. Eng.* **2002**, *22*, 777−788.
(18) Nasr, M. R. J.; Givi, M. M. Modeling of crude oil fouling in preheat exchangers of refinery distillation units. *Appl. Therm. Eng.* **2006**, *26*, 1572−1577.
(19) Lestina, T.; Zettler, G. U. Crude Oil Fouling Research: HTRI's Perspective. *Heat Transfer Eng.* **2014**, *35*, 217−223.
(20) Saunders, E. A. D. *Heat Exchangers: Selection, Design & Construction*; Longman Scientific & Technical: 1988.
(21) Diaz-Bejarano, E.; Coletti, F.; Macchietto, S. Crude oil fouling deposition, suppression, removal − and how to tell the difference. Presented at *Heat Exchanger Fouling and Cleaning Conference*, Dublin, Ireland, 2015.
(22) Ishiyama, E. M.; Heins, A. V.; Paterson, W. R.; Spinelli, L.; Wilson, D. I. Scheduling cleaning in a crude oil preheat train subject to fouling: Incorporating desalter control. *Appl. Therm. Eng.* **2010**, *30*, 1852−1862.
(23) Ishiyama, E. M.; Paterson, W. R.; Wilson, D. I. Thermo-hydraulic channeling in parallel heat exchangers subject to fouling. *Chem. Eng. Sci.* **2008**, *63*, 3400−3410.
(24) Incropera, F. P.; DeWitt, D. P.; Bergman, T. L.; Lavine, A. S. *Fundamentals of Heat and Mass Transfer*, 6th ed.; John Wiley & Sons: 2006.
(25) TEMA. *Standards of the Tubular Exchanger Manufacturers Association*, 9th ed.; 2007.
(26) Costa, A. L. H.; Tavares, V. B. G.; Borges, J. L.; Queiroz, E. M.; Pessoa, F. L. P.; Liporace, F. S.; de Oliveira, S. G. Parameter estimation of fouling models in crude preheat trains. *Heat Transfer Eng.* **2013**, *34*, 683−691.
(27) Liporace, F. S.; de Oliveira, S. G. Real time fouling diagnosis and heat exchanger performance. *Heat Transfer Eng.* **2007**, *28*, 193−201.

DOI: 10.1021/acs.iecr.6b03564
Ind. Eng. Chem. Res. 2017, 56, 4377−4385